

# Analysis and Design of Low-Loss Planar Microwave Baluns Having Three Symmetric Coupled Lines

Jong-Wook Lee and Kevin J. Webb

School of Electrical and Computer Engineering  
Purdue University, West Lafayette, IN 47907-1285

**Abstract**— The bandwidth of the Marchand balun is analyzed as a function of design parameters using a simple model, which provides the analytical design basis for the planar three-coupled-line balun. Analytical and numerical results are presented to facilitate balun design. Using this approach, a low loss planar microstrip balun was designed, fabricated and tested. The measured balun insertion loss for one example was less than 0.5 dB over a 8 - 13 GHz band, with 3-dB bandwidth 6.5 - 16 GHz.

## I. INTRODUCTION

Balanced line operation is widely used, such as in antenna, mixer and push-pull amplifier applications. For an unbalanced interface to a balanced signal, the three-symmetric-coupled line balun has been used in mixers [1] and push-pull amplifiers [2]. These low-loss, broadband results used the compensated concept of Marchand with shorted resonators [3]. The three-symmetric-line balun is planar and simpler to fabricate and design than multi-layer coupled-line structures, and has the desirable property of increased coupling over a two-line system for fixed interline spacing. For the coupled line Marchand-type balun design, analytical methods based on the coupled line approach have been reported for analysis and synthesis [4], [5].

In this paper, we propose an analytic and numerical synthesis approach for a planar microstrip Marchand-type balun using a three conductor system, given bandwidth and input/output impedance requirements. Three design options that can be tailored for specific design requirements are identified and verified using a numerical approach.

## II. BALUN IMPEDANCE AND BANDWIDTH ANALYSIS

The three conductor coupled microstrip balun can be analyzed by considering the correlation between the coupled microstrip balun and coaxial balun of Fig. 1(a). Figure 1(b) is the coaxial balun redrawn from Fig. 1(a). Figure 1(c) shows a microstrip balun realized with a three-coupled-line system. The center conductor with impedance  $Z_b$  forms an open-terminated line in a CPW-like mode, and the outer conductors with impedance  $Z_{ab}/2$  are ground resonators across the balanced line. The line lengths are approximately one quarter wavelength at the center frequency. The quarter wavelength transformer with impedance  $Z_a$  can be used for additional impedance transformation, which can reduce in-band reflection.

The Marchand balun is used for broadband impedance matching from unbalanced impedance  $Z$ , to balanced impedance  $R$ . From the equivalent circuit shown in Fig. 1(b), assuming TEM lines in a homogeneous medium with

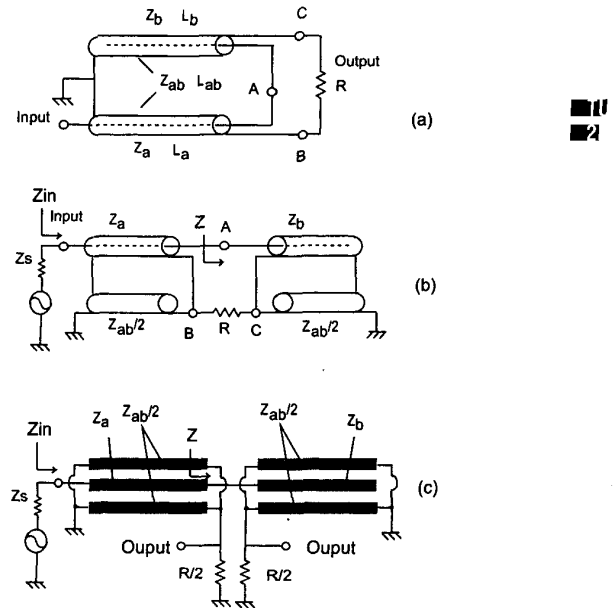


Fig. 1. (a) Coaxial balun schematic. (b) Equivalent circuit for calculation of impedance  $Z$  looking into nodes A-B. (c) Microstrip balun implementation using three-coupled-lines.

equal line lengths ( $L_a = L_b = L_{ab}$ ), the frequency-dependent impedance,  $Z(f)$ , looking into nodes A-B can be written in terms of real and imaginary parts as

$$\begin{aligned} Re[Z(f)] &= \frac{R}{1 + (\frac{R}{Z_{ab}})^2 \cot^2(\theta)}, \\ Im[Z(f)] &= \frac{\cot \theta \left[ \frac{R^2}{Z_{ab}} (1 - \frac{Z_b}{Z_{ab}} \cot^2 \theta) - Z_b \right]}{1 + (\frac{R}{Z_{ab}})^2 \cot^2(\theta)}, \end{aligned} \quad (1)$$

where  $\theta = (\frac{\pi}{2} \frac{f}{f_0})$ , and  $f_0$  is the band center frequency with the electrical length equal to one quarter wavelength. The input impedance,  $Z_{in}(f)$ , can be obtained by transforming  $Z(f)$  through a line section with impedance  $Z_a$ . The impedance  $Z_a$  is assumed to be same as  $Z_s$  with no impedance transformation in the following analysis. If we define bandwidth as the frequency range over which the impedance match is achieved within a specified reflection coefficient,  $|\Gamma_m|$ , using  $Z(f)$ ,

$$|\Gamma_m| = \left| \frac{Z(f_m) - Z_a}{Z(f_m) + Z_a} \right|. \quad (2)$$

The balun fractional bandwidth is defined as

$$BW = \frac{\Delta f}{f_0} = \frac{2(f_0 - f_m)}{f_0} = 2 - \frac{4\theta_m}{\pi}, \quad (3)$$

where  $f_m = \left(\frac{2\theta_m f_0}{\pi}\right)$  is the frequency where the reflection coefficient is equal to  $|\Gamma_m|$ .

Depending on the impedances selected for the structure, various reflection coefficients with different bandwidths are possible. Based on the relationship between impedances, we identify three different balun bandwidth and impedance categories. We call these Types I, II, and III. These types are analyzed assuming coaxial TEM modes.

For the Type I balun, the minimum reflection occurs at the balun center frequency,  $f_0$ , with  $R = Z_a$ . The impedance at  $f_0$  is perfectly matched independent of  $Z_b$  and  $Z_{ab}$ , and the real and imaginary parts of  $Z$  can be obtained by substituting  $R$  for  $Z_a$  in (1). The reactance is controlled with  $Z_b$  and  $Z_{ab}$ . If  $R = Z_{ab}$ , using (1)

$$Z(f) = Z_a \sin^2\left(\frac{\pi f}{2 f_0}\right) + j \cot\left(\frac{\pi f}{2 f_0}\right)(Z_a \sin^2\left(\frac{\pi f}{2 f_0}\right) - Z_b). \quad (4)$$

Using (4) and (2), an analytic bandwidth expression can be obtained by solving the following equation for  $\theta_m = \left(\frac{\pi f_m}{2 f_0}\right)$ :

$$A(\sin^2 \theta_m)^2 + B(\sin^2 \theta_m) + C = 0, \quad (5)$$

where  $A = 2ab + 3b - 2a + 1$ ,  $B = (a^2 + 2a - 1)(1 - b)$ , and  $C = -a^2(1 - b)$ , with  $a = \frac{Z_a}{R}$  the impedance ratio and  $b = |\Gamma_m|^2$ .

The Type II balun uses

$$Z_a = Z_b = R \sin^2 \theta_{1,2}, \quad Z_{ab} = R, \quad (6)$$

where the input/output impedance ratio determines the perfectly matched frequencies,  $f_1$  and  $f_2$ , and  $\theta_1 = \left(\frac{\pi f_1}{2 f_0}\right)$  and  $\theta_2 = \left(\frac{\pi f_2}{2 f_0}\right)$  are symmetrically located below and above  $f_0$  [6]. The imaginary part of  $Z$  is equal to zero at  $f_1$ ,  $f_2$ , and  $f_0$ . The impedance  $Z$  is perfectly matched to  $R$  at  $f_1$  and  $f_2$ , and is approximately matched over the band. The bandwidth is increased due to the compensating nature, where a match at the band center is sacrificed with reflection coefficient equal to  $(\frac{R - Z_a}{R + Z_a})$ . An analytical bandwidth expression is obtained by solving the following equation for  $\theta_m = \left(\frac{\pi f_m}{2 f_0}\right)$ :

$$A(\sin^2 \theta_m)^2 + B(\sin^2 \theta_m) + C = 0, \quad (7)$$

where  $A = 4ab + b - 1$ ,  $B = 2a(1 - b)$ , and  $C = -a^2(1 - b)$ , with  $a = \frac{Z_a}{R}$  being the input/output impedance ratio and  $b = |\Gamma_m|^2$ .

In the Type III balun, the bandwidth can be increased subject to the limit of  $Z_{ab}$  by choosing  $Z_b = \frac{R^2}{Z_{ab}}$  in (1). This condition results in zero reactance slope at the center frequency [7], which is known as the Marchand condition. The bandwidth can be large if a high  $Z_{ab}$  can be obtained, although the band center reflection increases with input/output impedance transformation ratio. The

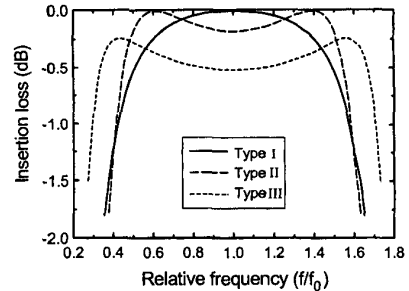


Fig. 2. Comparison of insertion loss of three types of baluns.

bandwidth is obtained by solving the following equation for  $\theta_m = \left(\frac{\pi f_m}{2 f_0}\right)$ :

$$A(\cot^2 \theta_m)^3 + B(\cot^2 \theta_m)^2 + C(\cot^2 \theta_m) + D = 0, \quad (8)$$

where  $A = a^3(1 - b)$ ,  $B = a^2c^2(1 - b)$ ,  $C = -2ac(1 - c + b + bc)$ , and  $D = (1 - c)^2 - b(1 + c)^2$ , with  $a = \left(\frac{R}{Z_{ab}}\right)^2$ ,  $b = |\Gamma_m|^2$ , and  $c = \frac{Z_a}{R}$  the input/output impedance ratio.

An example of the three balun specifications described above is summarized in the Table I. The bandwidth (BW) was calculated assuming that the minimum in-band reflection,  $|\Gamma_m|$ , is -10 dB. The  $|\Gamma_C|$  is the band center reflection. The calculated insertion losses for the three baluns are shown in Fig. 2.

TABLE I  
THREE BALUN DESIGN SPECIFICATIONS.

-	$Z_a$	$Z_b$	$Z_{ab}$	$R$	$BW$	$ \Gamma_C (dB)$
Type I	50	50	120	50	0.91	-40
Type II	70	70	100	100	1.08	-15
Type III	30	30	120	60	1.33	-10

### III. THREE-SYMMETRIC-COUPLED MICROSTRIP LINE BALUN DESIGN

After obtaining characteristic impedances based on bandwidth and input/output impedance, the coupled line dimensions in the planar microstrip structure are synthesized using a numerical approach. Only two of the three propagating modes in the three-line system ( $Z_{oo}$ ,  $Z_{ee}$ ,  $Z_{oe}$ ) [8] contribute, as the air-bridges eliminate the odd current mode  $Z_{oe}$ .

TABLE II  
The balun dimensions for three design specifications.

Dim. (μm)	$W_1$	$W_2$	$S$	$L_b$	$L_{ab}$
Type I	80	80	20	2550	2400
Type II	50	120	25	2500	2400
Type III	180	100	5	2600	2650

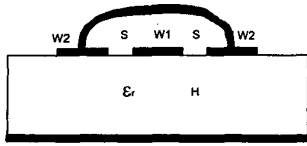


Fig. 3. Cross-sectional view of the symmetric-three-coupled line system with an air bridge.

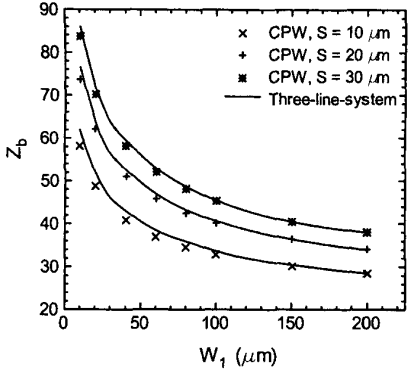


Fig. 4. Calculated impedance,  $Z_b$ , using the coplanar (CPW) mode for the three-coupled-line system with air bridge, as a function of  $W_1$ .  $H = 375 \mu\text{m}$ , AlN ( $\epsilon_r = 8.8$ ) is assumed, and  $W_2 = 100 \mu\text{m}$ .

The characteristic impedances for a given 2-D structure, shown in Fig. 3, were evaluated numerically for particular  $W_{1,2}$ ,  $S$ , and  $H$  values using the Agilent Advanced Design System [9]. Figure 4 shows the calculated characteristic impedance  $Z_b$ , i.e., the CPW mode, as a function of  $W_1$  for different spacings,  $S$ , using  $H = 375 \mu\text{m}$ ,  $\epsilon_r = 8.8$ , and  $W_2 = 100 \mu\text{m}$ , at 12 GHz. The characteristic impedance of the center conductor is similar to the CPW mode impedance because of the tight coupling between coupled lines. As a result, the dimensions  $W_1$  and  $S$  for  $Z_b$  can be determined almost independent of  $W_2$ . Figure 5 shows the calculated  $Z_{ab}/2$  as a function of  $W_2$  for various substrate thicknesses with  $S = 20 \mu\text{m}$ ,  $W_1 = 100 \mu\text{m}$ , and the other parameters the same as for the  $Z_b$  calculation. The change of characteristic impedance for different spacings was small when  $W_1$  was large compared to  $S$ . Therefore, a relatively large dimension  $W_1$ , compared to  $S$ , allowed us to choose  $W_2$  independent of  $S$ .

Using the balun specification of Table I, Fig. 4 and Fig. 5, the dimensions for the three types of balun were obtained, as shown in Table II. The substrate is 375  $\mu\text{m}$  thick with  $\epsilon_r = 8.8$ ,  $L_b$  is the open stub length, and  $L_{ab}$  is the grounded resonator length. The lengths were optimized considering the different phase velocities in coupled line modes. For the three balun designs,  $S$ -parameters were calculated using the ideal model (ID), the 2-D cross-sectional structure (2D), and a full-wave EM simulation (MOM). For the ideal calculation, the impedance values in Table I were used. In the 2-D calculation, different mode phase

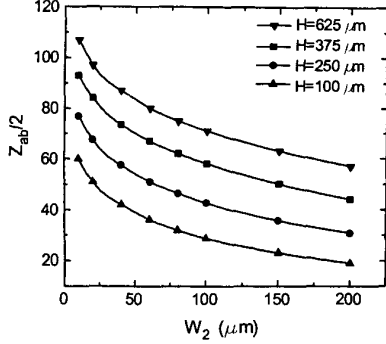


Fig. 5. Calculated impedance,  $Z_{ab}/2$ , for the three-coupled-line system with air bridge as a function of  $W_2$ , for various substrate thicknesses  $H$ .  $S = 20 \mu\text{m}$ ,  $W_1 = 100 \mu\text{m}$ .

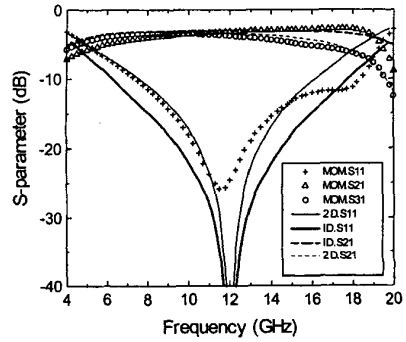


Fig. 6.  $S$ -parameters calculated for the Type I balun using the ideal model (ID), the 2-D cross-sectional structure (2D), and Momentum (MOM).

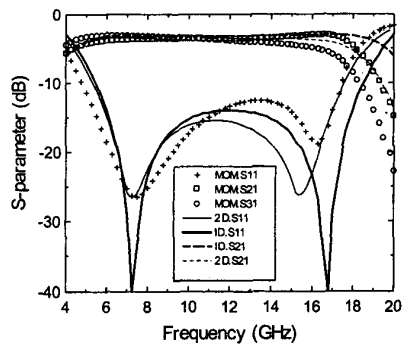


Fig. 7.  $S$ -parameters calculated for the Type II balun.

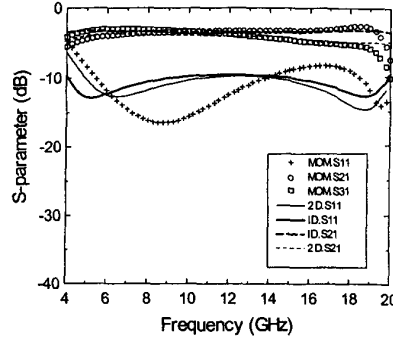


Fig. 8. *S*-parameters calculated for the Type III balun.

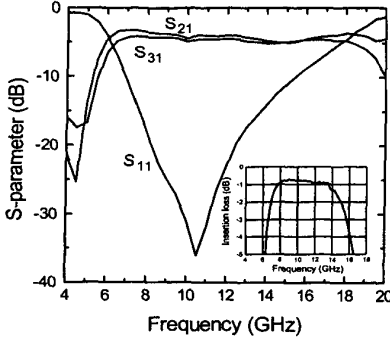


Fig. 9. Measured 3-port *S*-parameters of the balun. Measured insertion loss of the back-to-back balun is shown in the inset.

velocity, dispersion of effective dielectric constant, and conductor/dielectric loss were considered. The full-wave EM simulation was performed on an actual layout which included measurement port and via pad. The full-wave EM simulation and the 2-D calculation were done using Agilent ADS [9].

Figure 6 shows *S*-parameters calculated for the Type I balun using the three methods, showing good agreement at the center frequency ( $f_0 = 12$  GHz). Minimum reflection can be obtained at the center frequency in the Type I design, which is useful for such applications as narrow-band tuned amplifiers. Figure 7 shows the Type II case, where a perfect impedance match in both real and imaginary part is achieved below and above the center frequency. For the Type III design, a good match over the bandwidth can be achieved due to the high  $Z_{ab}$ , as shown in Fig. 8.

#### IV. FABRICATION AND MEASURED RESULTS

The previous design method was applied to design a 6-18 GHz balun with  $f_0 = 12$  GHz,  $50\ \Omega$  input and  $50\ \Omega$  output. An AlN substrate ( $\epsilon_r = 8.8$ ) of thickness  $375\ \mu\text{m}$  was used with  $2.5\ \mu\text{m}$  thick gold metalization. To characterize a 3-port balun using a 2-port measurement, the remaining output port was terminated with a  $25\ \Omega$  resistor. The measured 3-port *S*-parameters are shown in Fig. 9. For insertion loss assessment, two baluns were cascaded in a

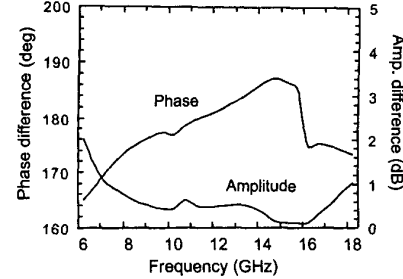


Fig. 10. Measured amplitude and phase balance.

back-to-back configuration, which resulted in less than  $0.5\ \text{dB}$  loss for each balun over 8-13 GHz, and 3-dB bandwidth of 6.5-16 GHz, as shown in the inset of Fig. 9. The amplitude balance,  $\text{dB}(|S_{21}|) - \text{dB}(|S_{31}|)$  and the phase balance,  $180^\circ - |\angle(S_{21}) - \angle(S_{31})|$ , of the output ports are shown in Figure 10, indicating less than 1 dB amplitude and  $\pm 10^\circ$  phase imbalance over 7-18 GHz.

#### V. CONCLUSION

Three balun design options having differing bandwidth were examined using an analytical method, and the design approach was verified using three numerical methods. A balun with excellent insertion loss, less than  $0.5\ \text{dB}$  over 8-13 GHz with a 3-dB bandwidth 6.5-16 GHz, was fabricated using the design method.

#### VI. ACKNOWLEDGMENTS

This work was supported by the Office of Naval Research under contracts #N00014-98-1-0371 and #N00014-96-1-1223, monitored by Dr. John Zolper.

#### REFERENCES

- [1] S. A. Maas and K. W. Chang, "A broadband, planar, doubly balanced monolithic Ka-band diode mixer," *IEEE Trans. Microwave Theory Tech.*, vol. 41, no. 12, pp. 2330-2335, Dec. 1993.
- [2] J. Schellenberg and H. Do-ky, "Low-loss, planar monolithic baluns for K/Ka-band application," in *IEEE MTT-S Int. Microwave Symp. Digest*, 1999, pp. 1733-1736.
- [3] N. Marchand, "Transmission-line conversion transformer," *Electronics*, vol. 17, no. 12, pp. 142-145, Dec. 1944.
- [4] M. Engels and R. H. Jansen, "Design of integrated compensated baluns," *Microwave and Optical Tech. Lett.*, vol. 14, no. 2, pp. 75-81, Feb. 1997.
- [5] K. S. Ang and I. D. Robertson, "Analysis and design of impedance-transforming planar Marchand baluns," *IEEE Trans. Microwave Theory Tech.*, vol. 49, no. 2, pp. 402-406, Feb. 2001.
- [6] W. K. Roberts, "A new wide-band balun," *Proceedings of the IRE*, vol. 45, pp. 1628-1631, Aug. 1957.
- [7] G. Oltman, "The compensated balun," *IEEE Trans. Microwave Theory Tech.*, vol. 14, no. 3, pp. 112-119, Mar. 1966.
- [8] V. K. Tripathi, "On the analysis of symmetric three-line microstrip circuits," *IEEE Trans. Microwave Theory Tech.*, vol. 25, no. 9, pp. 726-729, Sep. 1977.
- [9] Agilent Technologies, *Agilent Advanced Design System*, 2000.